Oxide Electronic Conductivity and Hydrogen Pickup Fraction in Zr alloys

Adrien Couet[a], Arthur T. Motta[a], Robert J. Comstock[b], Antoine Ambard[c]

[a]*Department of Mechanical and Nuclear Engineering, Penn State University, University Park, PA, USA, 16802*
(axc1019@psu.edu)
[b]*Westinghouse Electric Company, Pittsburgh, PA, USA, 15235*
[c]*EDF Research and Development, Materials and Mechanics of Components, Ecuelles, 77818 Moret-sur-Loing, France*

INTRODUCTION

The hydrogen pick-up during cladding corrosion is a critical life-limiting degradation mechanism for nuclear fuel in existing and advanced nuclear reactors, since hydrogen ingress can cause cladding embrittlement and limit cladding lifetime. However, mechanistic knowledge of the hydrogen pick-up mechanism is still lacking. This research investigates the mechanistic links between hydrogen pick-up, oxidation rate, alloy chemistry, and microstructure on a selection of zirconium alloys including, Zircaloy-4, ZIRLO®, Zr-2.5Nb, Zr-2.5Nb-0.5Cu and model alloys.

Hydrogen pick-up and oxide growth were precisely measured as a function of exposure time in an autoclave for a set of zirconium alloys with specific chemistries and microstructures [1, 2]. The results show that the instantaneous hydrogen pick-up fraction varies during corrosion, increasing just before oxide transition, when oxidation rate is the lowest [2]. Comparison between alloys has also shown that the alloying elements are closely related to the oxidation kinetics (and to the value of the corrosion exponent n) as well as to the hydrogen pick-up fraction [3]. As a result of these observations, it has been hypothesized that oxide electronic conductivity and alloying elements (either in precipitates or in solid solution) play key roles in the corrosion mechanism.

Oxide doping and the state of second phase precipitate particles when absorbed into the oxide layer have been studied by X-Ray Absorption Near Edge Spectroscopy (XANES). The results show that the oxidation state of the alloying elements varies with distance from the oxide metal interface and that the oxidation of second phase precipitates is delayed relative to the Zr matrix as previously shown [4]. Consequently oxide doping varies as a function of oxide position and exposure time [5]. However, the understanding of the specific effect of oxide doping on the zirconium oxide electronic conductivity is still lacking.

In the present study, the variation of the oxide electronic conductivity as function of exposure time and between alloys on various zirconium alloys presenting different oxide thickness and instantaneous hydrogen pickup fractions was measured using *in-situ* Electrochemical Impedance Spectroscopy (EIS). These conductivity measurements are compared with the evolution of hydrogen pickup fraction as function of exposure time to assess the possible correlation between oxide conductivity and hydrogen pickup fraction.

EXPERIMENTAL METHODS

This study focuses on the effect of oxide conductivity on hydrogen pickup fraction and oxidation kinetics of zirconium alloys. *In-situ* EIS experiments were performed to assess the oxide conductivity variations as function of exposure time and between alloy chemistry and compare it with the observed hydrogen pickup fraction variations.

In-Situ Electrochemical Impedance Spectroscopy

Impedance spectra of archived samples of various zirconium alloys corroded at 633 K in pure water were acquired. The oxide thickness and hydrogen pickup fraction of these samples have been previously measured before running the *in-situ* EIS experiments.

Fig.1 presents a schematic diagram of the EIS experimental setup. Electrical feedthroughs were provided by Pt wires in cooled Teflon seal elements at the top of the autoclave. Tube shaped zirconium samples served as the working electrode. A perforated Pt cylinder served as coaxial reference electrode for an approximate distance of 0.5mm between the electrodes leading to a symmetrical two-electrode configuration. Tube ends were isolated with spring-loaded Al_2O_3 ceramics exposing an outer surface area of about 6 cm^2. A Pt/Pt dummy cell of identical geometry was used for electrolyte conductivity monitoring. The contribution of the Pt electrode to the total impedance of the Zr/Pt cell measured with the dummy cell consisting of two electrodes in series is negligible.

Autoclave EIS measurements were taken at the open-circuit potential at frequencies about 10^{-4} to 10^6 Hz in a floating configuration (U_{ac} = 50mV) with a PAR4000 potentiostat. An example of Bode plots acquired on a Zircaloy-4 sample is shown in Fig.2. The shapes of the plots are similar to that observed in previous experiments [6]. Spectra are highly dispersive and, as seen after correction for the series electrolyte term (filled symbols in Fig.2), at higher frequencies they are dominated by the capacitive contribution of the oxide.
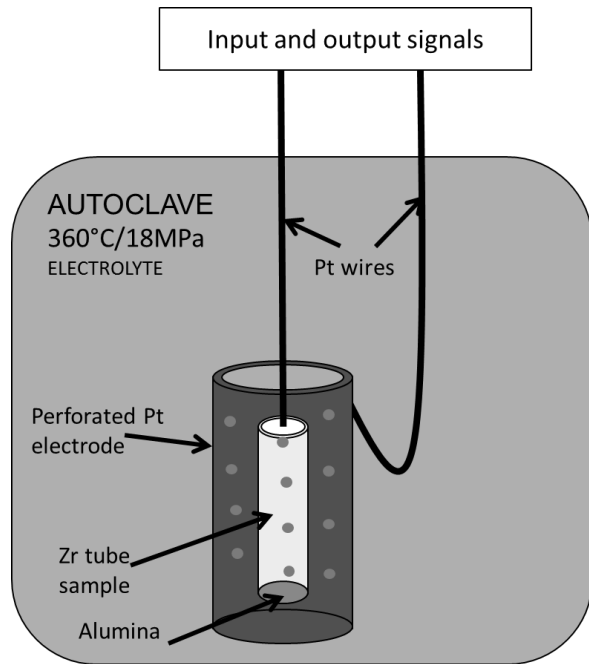
Fig. 1. Schematic diagram of the in-situ EIS experimental setup

Indeed the oxide layer at high frequencies can be considered as a pure capacitor. The real capacitance at high frequency can be related to the oxide thickness by the classical formula of a plane capacitor [6]:

$$\delta = \frac{\varepsilon(\omega)\varepsilon_0 S}{C(\omega)}$$

with δ the oxide thickness, ε the relative permittivity of ZrO_2, ε_0 the vacuum permittivity, S the sample surface and C the capacitance measured at a given frequency.

Since the oxide thickness can also be derived from the weight gain measurements, it is possible to verify the coherency of the EIS measurements.

It is observed in Fig.2 that the real impedance at low frequency tends towards a plateau as the phase tends toward zero indicating a pure resistive behavior of the system. The low frequency impedance of the system is thus a combination of the different resistances: the two interfacial resistances and the bulk oxide resistance (the distance between the two electrodes being small, the potential drop in the electrolyte is negligible as well as in the other parts of the electrical circuit). The oxide/metal interfacial resistivity is assumed to be negligible. Thus, in order to determine the bulk oxide resistance, one needs to evaluate the significance of the oxide/water interfacial resistance.

In order to evaluate the influence of the oxide/water interfacial impedance on the total impedance recorded at low frequency, EIS spectra of a pre-corroded Zircaloy-4 sample (δ~1µm) were acquired in electrolytes with different Li concentrations (2.2ppm, 4.4ppm and 8.8ppm).

It is indeed believed that Li should at least have an impact on the oxide/water interfacial reaction [7]. If no measurable influence of Li concentrations is observed on the low frequency impedance of the EIS spectra then one can be confident that the measured impedance is indeed solely due to the bulk oxide impedance and that the interfacial impedance is negligible.
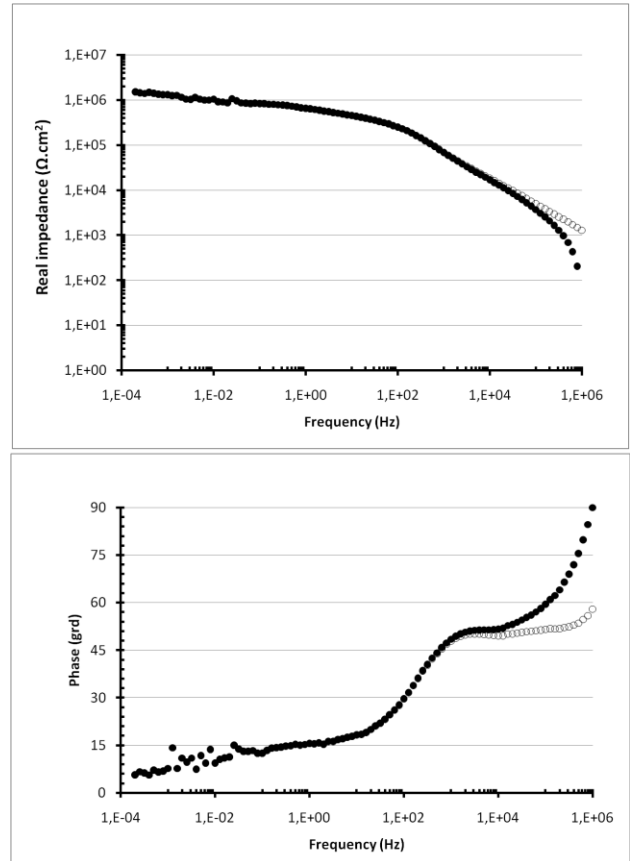

Fig. 2. Real impedance and phase as function of frequency of a Zircaloy-4 sample. The unfilled symbols are raw data, and the filled symbols are corrected for the electrolyte impedance.

RESULTS

The real impedance at low frequency is plotted in Fig.3 as function of different Li concentrations in the electrolyte. No significant influence of Li concentrations on the low frequency system impedance is observed, up to a concentration of 8.8ppm of Li. Thus the oxide/water interfacial impedance would be negligible and the measurement of the low frequency impedance is directly related to the bulk resistance of the oxide.
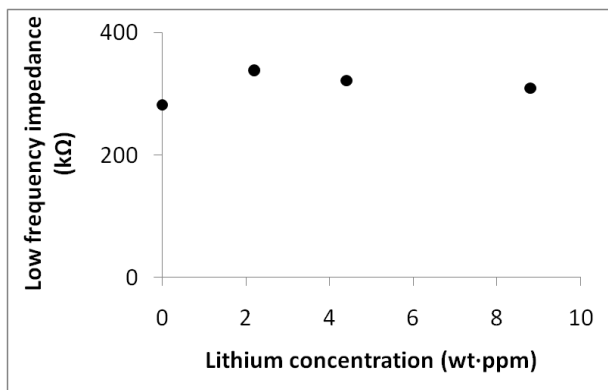
Fig. 3. Low frequency real impedance (average between 10^{-2} and 10^{-3}Hz) as function of Li concentrations in the electrolyte in Zircaloy-4.

The evolution of the weight gain deduced from the plane capacitor formula (ε=20) with the series capacitance (equal to $1/jZ\omega$) measured at 10kHz is plotted in Fig.4 (filled dots). The experimental weight gain and its power law fit ($w_g=kt^n$) are also plotted for comparison. The oxide transitions are also indicated at 130 days and 263 days of exposure.

Although one can observe significant scatter in the data, the evolution of the capacitance in series is similar to that of the weight gain (or oxide thickness).
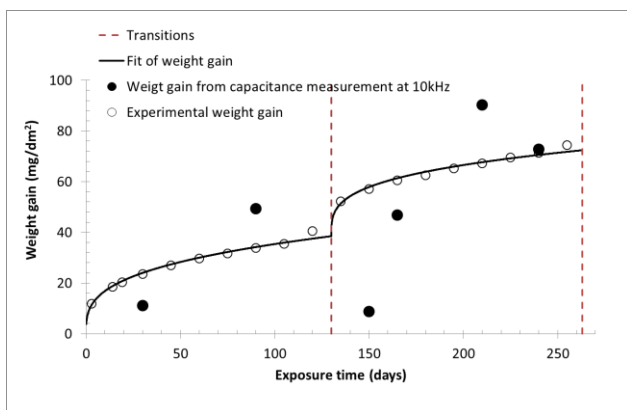

Fig. 4. Weight gain deduced from EIS spectra and from weight measurements in Zircaloy-4. The fit of the weight measurements and the transitions are also plotted [2].

The difference observed in the weight gain deduced from EIS spectra might come from the use of sister samples instead of a single sample in the EIS experiment. Also, a phase relaxation peak is observed at f=10kHz (see Fig.2) so that the derived capacitance might be affected by the evolution of the phenomenon related to this high frequency relaxation peak. Using a capacitance determined at a higher frequency (further away from this peak) would have also been delicate because of the removal of the series electrolyte term affecting the results in this frequency range. In any case, Fig.4 shows that

using the plane capacitor formula on sister samples is not an accurate method to accurately determine oxidation kinetics.

The oxide resistivity (ρ in Ω.cm) is calculated from low impedance measurements (Z) multiplied by a geometrical factor:

$$\rho = \frac{ZS}{\delta}$$

with the oxide thickness δ already deduced from weight gain data and S the sample surface. The oxide resistivity (in 10^6 Ω.cm) as function of exposure time is plotted in Fig.5. The instantaneous pickup fraction determined in another study [2] is also plotted for comparison and the oxide transitions are indicated.
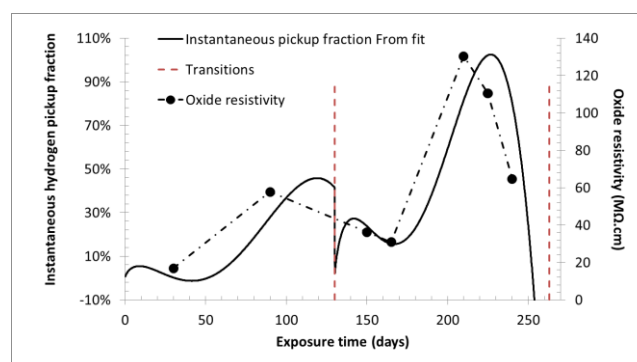

Fig. 5. Oxide resistivity and instantaneous hydrogen pickup fraction as function of exposure time in Zircaloy-4 [2].

The oxide resistivity is an oxide property, independent of its thickness. However, it is observed in Fig.5 that the resistivity varies as function of exposure time, indicating a change in oxide properties and in the resistance to electron transport of the oxide as the oxide grows. An apparent correlation is also observed between the oxide resistivity and the hydrogen pickup fraction indicating that the resistance to electron transport in the oxide is directly connected to hydrogen absorption. Basically, as the resistance to electron transport in the oxide increases, a greater driving force for proton absorption results, leading to a higher hydrogen pickup fraction. Thus, it seems reasonable to consider that the electrical potential across the oxide represents a significant driving force for hydrogen absorption into the underlying metal. The reasons for the alteration of electron transport in the oxide are not explicitly known. One possibility is that changes in oxide doping as the corrosion proceeds affect the oxide conductivity. It is indeed well established that the oxidation of alloying elements in precipitates and in solid solution in the oxide is delayed relative to the Zr matrix [5]. The presence of these unoxidized alloying elements leads to the emergence of new energy levels in the ZrO_2 band gap. Thus there would be a change in the untrapping

energy barriers for electrons through the oxide layer as function of exposure time affecting the electronic conductivity. Since the hydrogen pickup fraction is a strong function of the alloy, the evolution of oxide resistivity on single sister samples of Zircaloy-4, Zr-2.5Nb and Zr-2.5Nb-0.5Cu is currently being measured. The results should shed light on the influence of alloying elements on oxide conductivity.

REFERENCES

[1] A. Couet, A.T. Motta, R.J. Comstock, R.L. Paul, Cold neutron prompt gamma activation analysis, a non-destructive technique for hydrogen level assessment in zirconium alloys, *J. Nucl. Mater.*, Vol. 425, (2012), p. 211-217.
[2] A. Couet, A.T. Motta, R.J. Comstock, Hydrogen Pickup Measurements in Zirconium Alloys: Relation to Oxidation Kinetics, *J. Nucl. Mater.*, accepted.
[3] A. Couet, A.T. Motta, R.J. Comstock, Effect of alloying elements on hydrogen pick-up in zirconium alloys *17th International Symposium on Zirconium in the Nuclear Industry*, *ASTM STP 1543*, Hyderabad, India, 2013.
[4] D. Pêcheur, F. Lefebvre, A.T. Motta, C. Lemaignan, J.F. Wadier, Precipitate evolution in the Zircaloy-4 oxide layer, *J. Nucl. Mater.*, Vol. 189, (1992), p. 318-332.
[5] A. Couet, A.T. Motta, B. De Gabory, Z. Cai, X-Ray Absorption Near-Edge Spectroscopy study of Fe and Nb oxidation states evolution in Zircaloy-4, ZIRLO, Zr-2.5Nb and Zr-0.4Fe-0.2Cr oxide layers, *J. Nucl. Mater.*, , accepted.
[6] J. Schefold, D. Lincot, A. Ambard, O. Kerrec, The cyclic nature of corrosion of Zr and Zr-Sn in high-temperature water (633 K) - A long-term in situ impedance spectroscopic study, *Journal of The Electrochemical Society*, Vol. 150, (2003), p. B451-B461.
[7] M. Oskarsson, E. Ahlberg, K. Pettersson, Oxidation of Zircaloy-2 and Zircaloy-4 in water and lithiated water at 360 degrees C, *J. Nucl. Mater.*, Vol. 295, (2001), p. 97-108.